A NEW ANALYTICAL MODEL AND SENSORLESS APPROACH FOR SWITCHED RELUCTANCE MOTORS

S. Saha, T. Kosaka, N. Matsui   and   Y. Takeda

Dept. of Electrical & Computer Engg.
Nagoya Institute of Technology
Gokiso, Showa, Nagoya 466-8555, Japan

Dept. of Electrical & Electronics Systems Engg.
Osaka Prefecture University
1-1, Gakuencho, Sakai, Osaka,593 Japan

ABSTRACT - In this paper a new analytical model for the non-linear flux-linkage/ current characteristics of the switched reluctance motors at different rotor positions is proposed. The model has been successfully verified by the simulation and the experimental results of the instantaneous current waveforms and the average torque values in both single pulse and multiple pulse operation of the motor. The uniqueness of the model lies in its defining a simple algorithm for determining the rotor position (θ). Hence, sensorless operation of the motor can be easily implemented with the aid of this model.

1. INTRODUCTION

The chief feature of a switched reluctance motor (SRM) is its simple and rugged construction compared to that of a conventional ac machine. Hence, it is ideal for low cost and high speed drive systems in many industrial applications [1]. However, a traditional rotor position transducer is needed for its operation and here lies the major demerit. Therefore, to keep away the disadvantages of added expense, reliability problems, size and extra electrical connections associated with the rotor position transducer, different sensorless control schemes of the SRM have been proposed by several authors [2,3] over the recent years.

In the SRM, the flux linkage $\lambda(i, \theta)$ is a highly non-linear function of both the stator phase current (i) and the rotor position (θ). Hence, in the simplest SRM sensorless scheme, the flux-linkage (λ) together with the phase current (i) is first measured and subsequently, these two informations are used to determine the rotor position (θ) from the static magnetisation characteristics of the machine. Thus, accurate modelling of the flux-linkage/current characteristics of the machine with different rotor positions from the measured off-line data under static condition is mandatory for successful implementation of the sensorless scheme. However, during the actual operation of the machine, its characteristics may change from the static model due to unmodeled dynamics and change of machine parameters. For this reason, small error in determining the rotor position information (θ) using this principle cannot be ruled out. Therefore, this concept for the sensorless operation of the SRM holds good for an application

which does not require very precise control such as the compressor drive of an air-conditioning system.

Non-linear models of the SRM defining the relationship between the flux-linkage (λ), the phase current (i) and the rotor position (θ) have been developed using piecewise linearised approach, fuzzy logic and neural network techniques and the analytical methods. The accuracy of the reported several analytical models is quite good though retrieving the information of rotor position θ from them after measuring the on-line flux-linkage (λ) and the phase current (i) seems to be quite cumbersome. Therefore, in this paper a new analytical model is proposed so that the information of rotor position can be easily retrieved from it.

2. A GENERAL ANALYTICAL APPROACH FOR SRM MODELLING

In this section a general analytical expression defining the flux-linkage (λ) versus current (i) characteristics with different rotor positions (θ) is described. The analytical expression is of the form [4],

$$\lambda(i, \theta) = a_1(\theta)(1 - e^{a_2(\theta)i}) + a_3(\theta)i \qquad (1)$$

The authors in [4] were able to define the coefficients a_1, a_2 and a_3 by a Fourier cosine series of the form,

$$a_m = \sum_{k=0}^{\infty} A_{mk} \cos(k\alpha\theta) \qquad (2)$$

where θ is the mechanical angle of rotation and A_{mk} represents the kth Fourier coefficient of the mth fitting coefficient. The periodicity of the Fourier series is dependent on α, which is the number of electrical cycles per mechanical cycle seen by each phase. A rotor position of $0°$ corresponds to complete alignment for one of the phases. The quality of curve fit is reported to be good at all rotor positions when the coefficients a_1 to a_3 are represented by a Fourier series till the 8th harmonic.

The above discussed analytical expression of the SRM model is in the exponential form of phase current (i). Any sensorless scheme of the SRM demands

on-line real time calculation to determine the rotor position (θ). Hence, the SRM model in the exponential form has to be reduced to a polynomial equation in phase current (i) so that real time calculation becomes feasible. The assumption for the maximum power of this polynomial equation is a crucial factor in predicting the correct SRM model. Real time calculation also becomes difficult if a large number of higher order harmonics of the Fourier series have to be accommodated to define the coefficients of the above analytical equation.

3. A NEW MODELLING APPROACH FOR THE SRM

The basic concept of the new modelling approach consists of dividing the experimentally obtained off-line flux-linkage characteristics into two regions such as the unsaturated region (R1) and the saturated region (R2) as shown in Fig. 1. The phase current (i) at which the flux-linkage characteristics is divided into two regions is defined as i_d. The flux-linkage (λ) in the saturated and the unsaturated regions is now directly defined by a polynomial equation in phase current (i) and ($i - i_d$) respectively. The coefficients of the polynomial equations are expressed by a Fourier cosine series in rotor position (θ). For fast real time calculation, an effort has been made to restrict the power of the polynomial equations and minimise the harmonic order of the Fourier cosine series.

A low power SRM of few kilowatts is chosen for the modelling. The model is verified for a phase voltage of 110 V. The specifications of the test motor are given in Table 1. In the first step, the experimental flux-linkage/current characteristics of the test motor is obtained for every 5 mechanical degree of the rotor position from completely aligned to unaligned position. For this purpose, a step voltage of 110 V is applied to one of the phase winding and from the measured current waveforms at each 5° interval the flux-linkage curves at different rotor positions are calculated in a step by
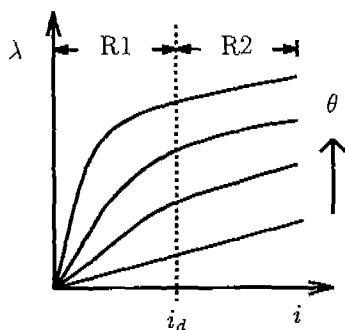

Fig. 1. Flux-linkage characteristics

Table 1. SRM Specifications

Stator pole no.	6
Rotor pole no.	4
Stator pole arc	30°
Rotor pole arc	45°
Stator outer diameter	$112mm$
Rotor outer diameter	$60.5mm$
Air gap length	$0.25mm$
Stack length	$80mm$
No. of turns per phase	80
Maximum phase current	$30A$

step fashion from the equation,

$$\lambda(n) = \lambda(n-1) + (V_s - i(n)R)T \tag{3}$$

where $\lambda(n)$ and $\lambda(n-1)$ are defined as the final and the initial value of flux-linkage over a discrete time step T when a constant voltage V_s is applied to a phase winding. i and R represent the current and phase resistance of a winding. The phase resistance of the motor is measured as 0.23 Ω.

Now, from the numerical curve fitting of the experimentally obtained flux-linkage versus current characteristics the analytical model of the SRM can be defined as follows. In the unsaturated region i.e. when $i \leq i_d$ the value of flux-linkage can be given by the polynomial equation,

$$\lambda_u(i, \theta) = \sum_{n=1}^{6} A_{un}(\theta)i^n \tag{4}$$

Coefficient $A_{un}(\theta)$ of the above equation is expressed in the Fourier cosine series form and can be defined as,

$$A_{un}(\theta) = \sum_{k=0}^{2} L_{unk} \cos(k\alpha\theta) \tag{5}$$

Similarly, in the saturated region i.e. when $i > i_d$ the value of flux-linkage can be given by the polynomial equation,

$$\lambda_s(i, \theta) = \sum_{n=1}^{6} A_{un}(\theta) \times i_d^n + \sum_{m=1}^{2} A_{sm}(\theta) \times (i - i_d)^m \tag{6}$$

The first part of the right hand side of the above equation is constant for a particular rotor position (θ) and hence defines the end points of the unsaturated region for different flux-linkage curves. The second part defines the saturated region. In an identical way, $A_{sm}(\theta)$ can be defined as,

$$A_{sm}(\theta) = \sum_{k=0}^{2} L_{smk} \cos(k\alpha\theta) \tag{7}$$

The value of i_d for the test motor is 15 A. The chief feature of the proposed model lies in defining the
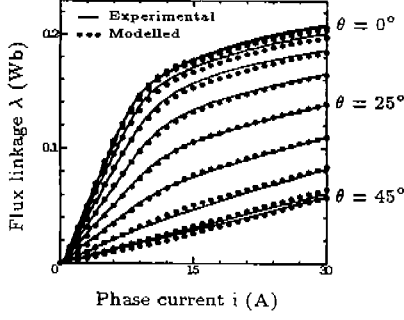
Fig. 2. Final modelling result

Fig. 3. Incremental increase in rotor position when $i < i_d$

Fourier cosine series of the two coefficients $A_{un}(\theta)$ and $A_{sm}(\theta)$ after discrete Fourier transform (DFT) analysis. For both the coefficients, the Fourier cosine series is restricted only up to the second harmonic component and here lies the simplification of our modelling approach. Finally, with the help of (4), (5), (6) and (7) the flux linkage curves at all the rotor positions are plotted in Fig. 2 and are shown as dotted lines. The firm lines in Fig. 2 depicts the experimental flux-linkage curves. From this figure, it is observed that the flux-linkage curves obtained analytically are well matched with those obtained experimentally. A percentage error analysis of the analytical and the experimental flux-linkage data for a given current at all rotor positions shows that the deviation between the two data is within 5 %.

4. INSTANTANEOUS CURRENT AND TORQUE CALCULATION

Instantaneous current at constant speed can be calculated from the numerical solution of (4) or (6) defining the flux-linkage current characteristics and (3) defining the rate of change of flux-linkage in a winding. The flux-linkage value (λ_u) in (4) or the (λ_s) in (6) is substituted by the value of (λ) from (3) and the resultant equation with phase current (i) as the variable is solved by Newton-Raphson method. The starting values of (λ) and the phase current (i) for the solution of this equation are zero. At every incremental step the flux-linkage value (λ) is updated and the new phase current value (i) is obtained. This phase current value (i) at every instant also helps to determine the instantaneous torque which is defined by,

$$T = [\frac{dW}{d\theta}]$$ (8)

where dW is the incremental change in co-energy and $d\theta$ is the incremental change in rotor position. For an infinitesimal change of $d\theta$ in rotor position the phase current value (i) can be assumed to be constant. The incremental change in co-energy when the rotor moves
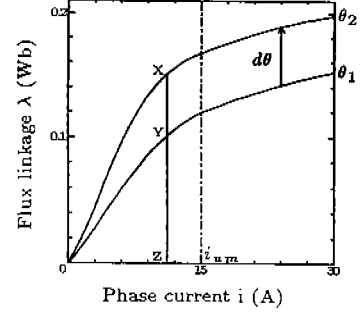
from position (θ_1) to (θ_2) is given by,

$$dW = \int_0^i [\lambda(i, \theta_2) - \lambda(i, \theta_1)]di$$ (9)

where $\lambda(i, \theta_2)$ and $\lambda(i, \theta_1)$ define the flux-linkage values at rotor position θ_2 and θ_1 respectively. The incremental change in co-energy dW_u in the unsaturated region (i.e . $i < i_d$) can be explained from Fig. 3 and is derived as follows:

$$dW_u = OXY = OXZ - OYZ$$

$$dW_u = \sum_{n=1}^{6} \frac{i^{n+1}}{n+1}[A_{un}(\theta_2) - A_{un}(\theta_1)]$$ (10)

Similarly, the incremental change in co-energy dW_s in the saturated region (i.e. above i_d) can be explained from Fig. 4 and is expressed as:

$$dW_s = ODF = ODH - OFH$$
$$= (OAC - OBC) + (ADHC - BFHC)$$
$$= (OAC - OBC) + (ADE - BFG)$$
$$+ (AEHC - BGHC)$$

$$dW_s = \sum_{n=1}^{6} \frac{i_d^{n+1}}{n+1}[A_{un}(\theta_2) - A_{un}(\theta_1)]$$
$$+ \sum_{n=1}^{2} \frac{(i - i_d)^{n+1}}{n+1}[A_{sn}(\theta_2) - A_{sn}(\theta_1)]$$
$$+ (i - i_d) \times \sum_{n=1}^{6} i_d^n[A_{un}(\theta_2) - A_{un}(\theta_1)]$$

(11)

From the above discussion it is clear that the instantaneous phase current and torque calculations of the SRM can be easily done with the help of the proposed analytical model. Simulations for the instantaneous phase current and torque of the test motor with the help of these equations are carried out and are reported in the next section.
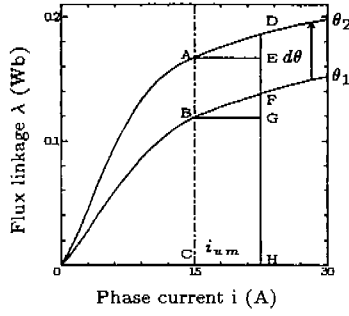
Fig. 4. Incremental increase in rotor position when $i > i_d$

5. VERIFICATION OF THE PROPOSED MODEL

The proposed model has been verified with simulation and experimental results of the instantaneous current waveforms and the average torque values in both single pulse and multiple pulse operation of the test motor. For the single pulse operation, it is considered that the motor is rotating at a constant speed of $3000rpm$ and the turn on angle (θ_o) and the commutation angle (θ_c) are 45 and 67 mechanical degree respectively. The voltage V_s applied to the phase winding is $110V$. At the instant of commutation -110 V is immediately applied to the phase winding. Similarly, for the multiple pulse operation, the constant motor speed is chosen as $2000rpm$ and the turn on angle (θ_o) and the commutation angle (θ_c) are selected as 45 and 71.9 mechanical degree respectively. In this case, at the instant of turn on 110 V is applied across the phase winding and the phase current of the motor is sensed every $90.5\mu s$ so that when its value goes above 20 A the phase voltage applied across the winding changes from 110 V to -110 V. Now when the phase current falls below 20 A, 110 V is again reapplied to the phase winding. The process repeats until -110 V is finally applied to the phase winding at the instant of commutation.

The experimental drive circuit of the SRM is shown in Fig. 5 and is self-explanatory. The simulated and the experimental instantaneous current waveforms in the single pulse operation are shown in Fig. 6. The
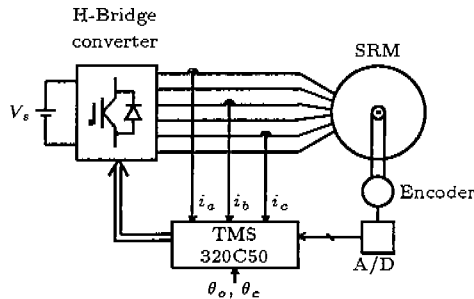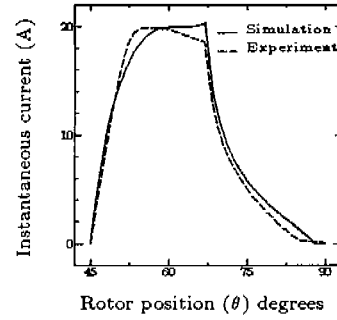

Fig. 5. Experimental system

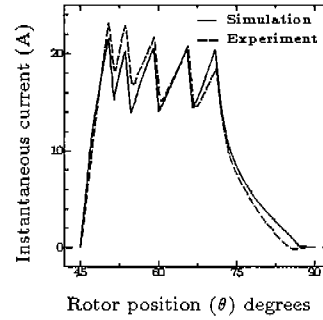Fig. 6. Instantaneous current waveform in single pulse operation

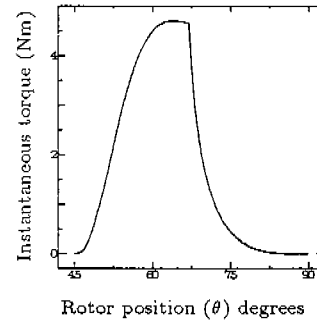Fig. 7. Instantaneous current waveform in multiple pulse operation

Fig. 8. Simulated instantaneous torque waveform in single pulse operation

top of the experimental current waveform is not flat as the simulated one because the capacitor voltage which is an input to the H-bridge converter circuit drops by 3 V. Other than this the simulated and the experimental current waveform are well matched. Similarly, the simulated and the experimental instantaneous current waveforms in the multiple pulse operation are shown in Fig. 7 and are found to be closely matched. The simulated instantaneous torque waveform in the single pulse and the multiple pulse operation are also shown in Fig. 8 and Fig. 9 respectively. The experimental instantaneous torque waveforms are not obtained because of the limited frequency band of the torque transducer. Hence, for both the single pulse and the multiple pulse operation the values of average torque are calculated from the simulated results of the instantaneous torque
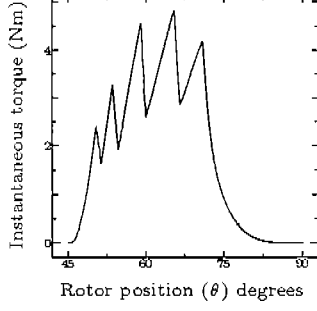
Fig. 9. Simulated instantaneous torque waveform in multiple pulse operation

waveforms and are compared with the observed experimental values. For the single pulse operation, the simulated and the experimental average torque values are 2.5 and 2.6Nm respectively, whereas in the multiple pulse operation they are 2.65 and 2.7Nm respectively. The above results clearly proves the validity of the proposed model.

6. SENSORLESS APPROACH

The successful verification of the proposed SRM model supports the implementation of the sensorless operation of the motor using its aid. The first step in the implementation of any sensorless scheme calls for retrieving the information of rotor position (θ) from the measured values of the flux-linkage (λ) and the phase current (i). Hence, in this section, it has been highlighted that how the rotor position information (θ) can be easily determined from the proposed model.

Equations (4) and (5) together in section 3. define the flux-linkage curves in the unsaturated region. Now, if the value of the coefficient $A_{un}(\theta)$ from (5) is substituted in (4), it can be expressed as

$$A_1 \cos(2\alpha\theta) + B_1 \cos(\alpha\theta) + C_1 = 0 \qquad (12)$$

where A_1, B_1 and C_1 are given by,

$$A_1 = \sum_{n=1}^{6} L_{un2} i^n \qquad (13)$$

$$B_1 = \sum_{n=1}^{6} L_{un1} i^n \qquad (14)$$

$$C_1 = \sum_{n=1}^{6} L_{un0} i^n - \lambda_u \qquad (15)$$

After sensing the phase current i and the phase voltage V_s the flux-linkage λ_u in (15) can be calculated from the following expression,

$$\lambda_u = \int (V_s - iR) dt \qquad (16)$$

Hence, the values of A_1, B_1 and C_1 can be easily on-line computed in a digital signal processor from the information of phase current i and phase voltage V_s. Further (12) can be reduced to the form,

$$2A_1 \cos^2(\alpha\theta) + B_1 \cos(\alpha\theta) + (C_1 - A_1) = 0 \qquad (17)$$

The above equation is a quadratic equation in $\cos(\alpha\theta)$ and hence the value of rotor position (θ) when $i \leq i_d$ can be easily determined from it. In an identical way, the rotor position (θ) when $i > i_d$ can be determined and is explained as follows. In this case, the values of the coefficients $A_{un}(\theta)$ and $A_{sm}(\theta)$ from (5) and (7) are substituted in (6) so that it can be expressed as,

$$A_2 \cos(2\alpha\theta) + B_2 \cos(\alpha\theta) + C_2 = 0 \qquad (18)$$

where A_2, B_2 and C_2 are given by,

$$A_2 = \sum_{n=1}^{6} L_{un2} i_d^n + \sum_{m=1}^{2} L_{sm2}(i - i_d)^m \qquad (19)$$

$$B_2 = \sum_{n=1}^{6} L_{un1} i_d^n + \sum_{m=1}^{2} L_{sm1}(i - i_d)^m \qquad (20)$$

$$C_2 = \sum_{n=1}^{6} L_{un0} i_d^n + \sum_{m=1}^{2} L_{sm0}(i - i_d)^m - \lambda_s \qquad (21)$$

In a similar way the flux-linkage value λ_s can be calculated from (16). The first terms in the right hand side of (19), (20) and (21) are constant and can be stored in the memory of a processor. The second terms of these equations are on-line computed after sensing the phase current i. Therefore, in this case too, on-line computation of A_2, B_2 and C_2 can be done. Now, like the earlier case, (18) can be represented by a quadratic equation in $\cos(\alpha\theta)$ such as

$$2A_2 \cos^2(\alpha\theta) + B_2 \cos(\alpha\theta) + (C_2 - A_2) = 0 \qquad (22)$$

Solving the above quadratic equation, rotor position (θ) when $i > i_d$ can also be easily determined.

A first hand knowledge of the rotor position error $\Delta\theta$ between the actual measured rotor position (θ_m) and the estimated rotor position (θ_e) is very important before designing any sensorless scheme of the motor. Hence, a suitable experiment to obtain the rotor position error $\Delta\theta$ is in process. The flowchart in Fig. 10 shows how the rotor position error $\Delta\theta$ can be determined experimentally. In the first step, the aligned position of the 'U' phase is chosen as the reference $0°$ mechanical. Now, the dc link voltage V_c, all the phase currents i_u, i_v and i_w, and the actual rotor position (θ_m) are sensed. The rotor position is sensed by an encoder such that it generates four electrical cycles in one full mechanical cycle of $360°$. At some instant of time, two phases may be conducting simultaneously

Start

Select aligned position of 'U'
phase as the ref. 0° mechanical

Sense the dc link voltage V_c, all
the phase currents i_u, i_v, i_w and
measure actual rotor position θ_m

Compare magnitude of i_u, i_v and
i_w and select the effective phase

$\lambda_e = \int (v_s - i_e)dt$

$i_e > i_d$ No   Yes

Calculate A_1, B_1, and
C_1 as per Eq. (13),
(14) and (15)

Calculate A_2, B_2, and
C_1 as per Eq. (19),
(20) and (21)

Solve the quadratic
Eq. (17) and obtain
the value of $\cos(\alpha\theta)$

Solve the quadratic
Eq. (22) and obtain
the value of $\cos(\alpha\theta)$

From look-up table find the
estimated rotor position (θ_e)

For 'V' and 'W' phase add $-30°$
and $+30°$ respectively to θ_e
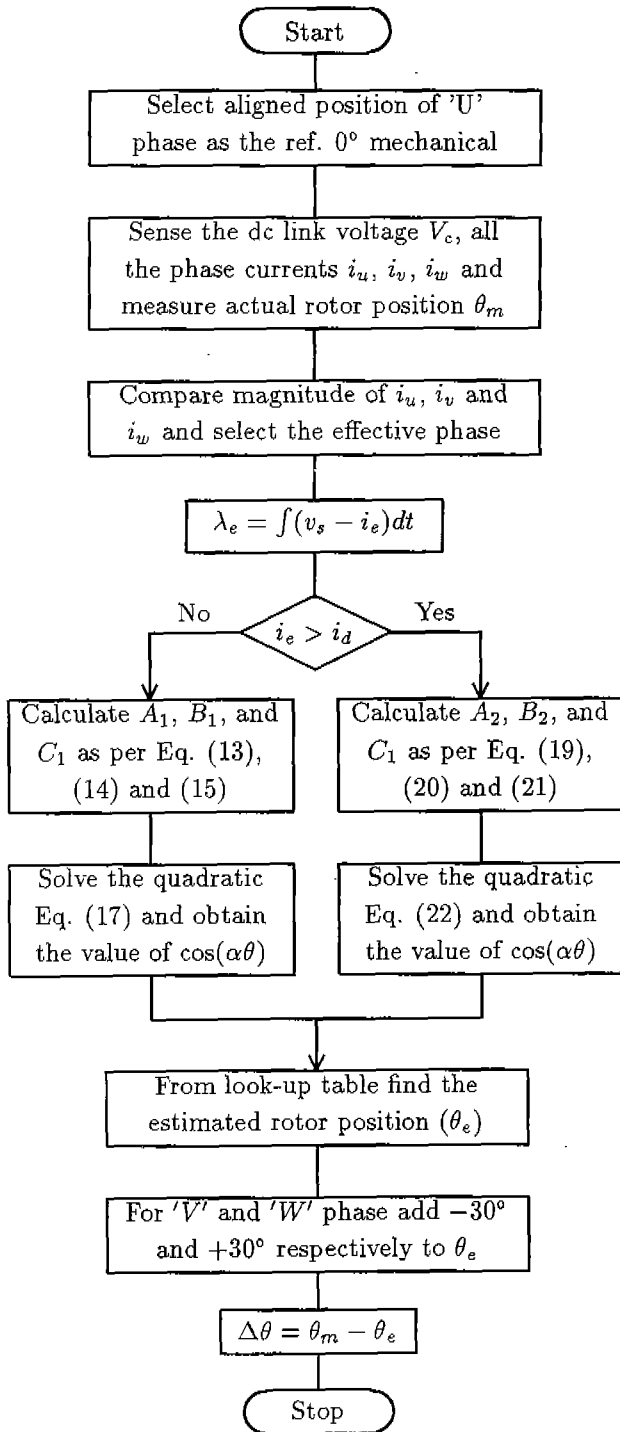
$\Delta\theta = \theta_m - \theta_e$

Stop

Fig. 10. Flow chart for calculating error $\Delta\theta$

and hence in the next step comparison of the magnitudes of all the phase currents are done so that the effective conducting phase can be selected. The phase which has the maximum value of current is the effective conducting phase. The instantaneous current of the effective conducting phase is defined as i_e. Now, from the measured dc link voltage V_c, the instantaneous phase voltage v_s is calculated considering the voltage drop across the power devices. After this the effective instantaneous flux-linkage λ_e value is calculated as shown in the flowchart. In the following step, the value of the effective phase current i_e is compared with i_d so that the estimated rotor position (θ_e) in both the unsaturated and the saturated region can be obtained from the look-up table stored in the memory of the processor after solving two different quadratic equations in $\cos(\alpha\theta)$. For the 'V' and 'W' phases $-30°$ and $+30°$ is added to the original value of the estimated rotor position (θ_e) respectively. The value of the estimated rotor position (θ_e) is made to reset after every 90° so that it can be easily compared with the actual measured rotor position (θ_m) to detect the rotor position error $\Delta\theta$. If a comparatively powerful CPU such as DSP TMS320C50 is used for on-line computation, it is expected that the rotor position error $\Delta\theta$ will be within reasonable limits.

7. CONCLUSION

Any low power SRM motor within the range of few kilowatts can be modeled through this simple approach wherein the flux-linkage characteristics is expressed by two polynomial equations-one for the unsaturated region and the other for the saturated region. The coefficients $A_{un}(\theta)$ and $A_{sm}(\theta)$ of these two equations are defined in the Fourier cosine series form. But the cosine series of both the coefficients is restricted only upto the second harmonic component. For these factors real time calculation for determining the rotor position (θ) with the help of this model will be very easy. Hence, developing a sensorless SRM drive with the aid of this model is a feasible concept.

REFERENCES

[1] T.J.E.Miller : Switched reluctance motor and their control, Magna physics publishing and Oxford university press, 1993.

[2] G-Lopez, P.C.Kjaer and T.J.E.Miller : A new sensorless method for switched reluctance motor drives, Proc. of IEEE/IAS Ann. Meeting, Vol.1, pp.564-570, 1997.

[3]M.T.DiRenzo and Wasim Khan : Self-trained commutation algorithm for SR motor drive system without position sensing, Proc. of IEEE/IAS Ann. Meeting, Vol.1, pp.341-348, 1997.

[4] D.A.Torrey and J.H.Lang : Modelling a nonlinear variable-reluctance motor drive, IEE proceedings, Vol. 137, Pt. B, No. 5, pp. 314-326, Sept. 1990.